

Emission of terahertz radiation from coupled plasmon-phonon modes in InAs

M. P. Hasselbeck,^{1,2} D. Stalnaker,¹ L. A. Schlie,¹ T. J. Rotter,³ A. Stintz,³ and M. Sheik-Bahae²

¹USAF Research Laboratory, Directed Energy Directorate, Kirtland AFB, New Mexico 87117

²Department of Physics and Astronomy, University of New Mexico, Albuquerque, New Mexico 87131

³Center for High Technology Materials, University of New Mexico, Albuquerque, New Mexico 87106

(Received 29 November 2001; published 29 May 2002)

Coherent electromagnetic radiation is generated by the oscillation of longitudinal modes associated with optical phonons and bulk plasmons in InAs. Dramatic changes to the radiation spectra occur when the plasmon and phonon frequencies are in close spectral proximity, i.e., when the modes become strongly coupled.

DOI: 10.1103/PhysRevB.65.233203

PACS number(s): 78.47.+p, 72.30.+q, 73.20.Mf

Plasmons and phonons represent fundamental collective excitations in solids. In polar materials, the plasmons, and longitudinal optical (LO) phonons can couple to form hybrid modes at new frequencies that were first observed by incoherent Raman scattering of continuous laser light from GaAs.¹ The availability of laser pulses with duration much shorter than the oscillation period of these modes allows impulsive excitation of coherent, macroscopic motion of charge carriers and lattice ions that can radiate into free space.² Emission of THz frequency electromagnetic radiation by coherent phonons³⁻⁵ and bulk plasmons⁶ has been reported, but only limited information exists for the situation where both modes are radiating. Recent experiments have provided evidence for THz emission from plasmon-phonon modes in InSb,⁷ InAs, and GaAs,⁸ but an investigation of how mode hybridization affects the radiation spectrum has, until now, not been available.

We present an experimental study of the free-space radiation originating from the longitudinal modes of a polar semiconductor as a function of coupling. We find that the THz frequency emission is governed by bulk plasma oscillations. Only when the longitudinal phonon vibrations approach resonance with the plasma frequency—the strong coupling regime—do they significantly affect the radiation spectrum. In addition, we observe that cold plasmons and phonons can radiate coherently even when interacting with an inhomogeneous, hot electron-hole plasma at a density several orders of magnitude higher than the background doping density. Our experimental results are reproduced by model calculations and confirm theoretical predictions of Kuznetsov and Stanton.⁹

Time-resolved measurements of coupled, coherent oscillations in polar semiconductors have been primarily made by reflective electro-optic sampling (REOS).¹⁰ These experiments are sensitive to electric field changes that occur in the narrow ($<1 \mu\text{m}$) surface space-charge region. An ultrashort laser pulse injects electron-hole pairs, which partially screen the surface field. Long-range Coulomb coupling of the ultrafast field transient to both the electronic polarization and the polar lattice can initiate collective oscillations, which weakly modulate the surface field as observed in reflection. A complication of REOS is that the plasma frequency is determined by the sum of the photocarrier and background carrier densities. Furthermore, REOS detects oscillations that are confined in the surface field layer; this has

been shown to limit the minimum plasmon wave vector in InAs.¹¹ Another approach is to measure the electromagnetic radiation emitted by coherent macroscopic dipoles in the bulk. Two popular detection techniques are optically gated antennas and free-space electro-optic sampling, which give the temporal phase of the THz pulse relative to the excitation pulse. Phase data can be helpful for elucidating the starting mechanism of the coherent oscillations, but these methods often exhibit dispersion and Reststrahl absorption at optical phonon frequencies in III-V semiconductors.^{12,13} Here, we use a phase-insensitive arrangement to make broadband measurements of the emitted radiation spectrum, which eliminates signal distortion problems in the spectral region of interest between 1-10 THz.

Our experiments are based on an interferometric technique used by Kersting *et al.* to study coherent plasmon oscillations in bulk GaAs.⁶ Two 30 fs pump pulses derived from a Ti:sapphire laser (center wavelength 770 nm) are focused on slightly separated spots on an InAs crystal ($E_g = 0.36 \text{ eV}$ at 300 K) at an incidence angle of 45° . Spatial separation of the pump pulses represents an important modification of the original setup; each excited spot generates an independent THz frequency pulse without complications from pump beam overlap.¹⁴ The THz pulses propagate into free space and are collected by an off-axis parabolic mirror, collimated, and spatially filtered. A second mirror focuses the two THz beams on a liquid-He cooled Si bolometer. By adjusting the relative time-delay of the two pump pulses, the detector signal maps out a linear interferogram of the electromagnetic transient emitted from the semiconductor. Although the THz pulses originate from spatially separate regions, their diffraction angle is sufficiently large to allow interference in the far field. The pump irradiance is kept low to suppress generation of far-infrared light by surface rectification.¹⁵ The InAs samples are of two types: (i) 0.5-mm and 1-mm-thick bulk LEC grown wafers oriented (111) or (100) and doped with S or Te and (ii) $\sim 1\text{-}\mu\text{m}$ -thick MBE layers doped with Si and grown on intrinsic (100) InAs substrates. Other than doping concentration, we could not identify any dependence on sample orientation or preparation method in the THz data.

Figure 1 displays (a) time-resolved linear interferograms and (b) corresponding Fourier-transform spectra obtained at room temperature with samples at four progressively higher donor densities while maintaining the same excitation irradi-

Report Documentation Page

Form Approved
OMB No. 0704-0188

Public reporting burden for the collection of information is estimated to average 1 hour per response, including the time for reviewing instructions, searching existing data sources, gathering and maintaining the data needed, and completing and reviewing the collection of information. Send comments regarding this burden estimate or any other aspect of this collection of information, including suggestions for reducing this burden, to Washington Headquarters Services, Directorate for Information Operations and Reports, 1215 Jefferson Davis Highway, Suite 1204, Arlington VA 22202-4302. Respondents should be aware that notwithstanding any other provision of law, no person shall be subject to a penalty for failing to comply with a collection of information if it does not display a currently valid OMB control number.

1. REPORT DATE 29 MAY 2002		2. REPORT TYPE		3. DATES COVERED 00-00-2002 to 00-00-2002	
4. TITLE AND SUBTITLE Emission of terahertz radiation from coupled plasmon-phonon modes in InAs				5a. CONTRACT NUMBER	
				5b. GRANT NUMBER	
				5c. PROGRAM ELEMENT NUMBER	
6. AUTHOR(S)				5d. PROJECT NUMBER	
				5e. TASK NUMBER	
				5f. WORK UNIT NUMBER	
7. PERFORMING ORGANIZATION NAME(S) AND ADDRESS(ES) USAF Research Laboratory, Directed Energy Directorate, Kirtland AFB, NM, 87117				8. PERFORMING ORGANIZATION REPORT NUMBER	
9. SPONSORING/MONITORING AGENCY NAME(S) AND ADDRESS(ES)				10. SPONSOR/MONITOR'S ACRONYM(S)	
				11. SPONSOR/MONITOR'S REPORT NUMBER(S)	
12. DISTRIBUTION/AVAILABILITY STATEMENT Approved for public release; distribution unlimited					
13. SUPPLEMENTARY NOTES					
14. ABSTRACT					
15. SUBJECT TERMS					
16. SECURITY CLASSIFICATION OF:			17. LIMITATION OF ABSTRACT	18. NUMBER OF PAGES	19a. NAME OF RESPONSIBLE PERSON
a. REPORT unclassified	b. ABSTRACT unclassified	c. THIS PAGE unclassified			

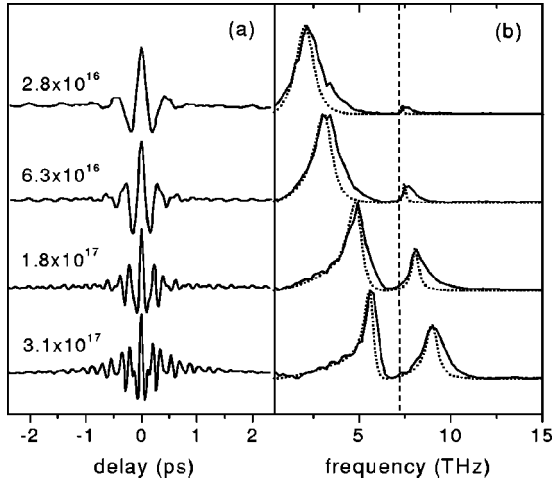


FIG. 1. (a) Time-resolved linear interferograms for bulk (100) n -doped InAs samples and (b) corresponding Fourier transform spectra (solid lines). Labeled doping densities are in units of cm^{-3} . The dashed vertical line indicates the bare LO phonon frequency. Dotted curves in (b) are calculated using Eq. (2).

ance. The top spectrum with a lightly n -doped bulk wafer reveals a broad plasma peak centered at $\nu_p = 2.1$ THz and a much weaker peak near the bare LO phonon frequency of $\nu_{\text{LO}} = 7.3$ THz (dashed vertical line for reference). As the donor density increases, three features are evident: (i) the plasma peak moves to higher frequency, (ii) coupling of the plasmon like to the phononlike mode strengthens causing a blueshift of the upper-hybrid mode, and (iii) the spectral weight of the upper-hybrid mode dramatically increases accompanied by significant broadening. The bottom spectrum, where the sample is doped to be very close to the anticrossing frequency (i.e., where $\nu_p = \nu_{\text{LO}}$), exhibits a pronounced shift of the upper-hybrid mode. The plasma frequency is just above the bare LO phonon frequency in this sample so we identify the upper-hybrid mode as the plasmonlike mode.

The spectral locations of both the upper- and lower-hybrid modes are explained by the concentration of ionized donor atoms in the bulk sample. The longitudinal mode frequencies of the coupled plasmon-phonon system are zeros of the dielectric response function in the weak damping, long wavelength limit, i.e., where

$$\epsilon_{\infty} \left(1 - \frac{\omega_p^2}{\omega^2} \right) + \frac{\epsilon_0 - \epsilon_{\infty}}{1 - \omega^2/\omega_{\text{TO}}^2} = 0. \quad (1)$$

The low- and high-frequency dielectric constants are $\epsilon_0 = 11.8$ and $\epsilon_{\infty} = 14.55$, respectively, $\omega_{\text{TO}}/2\pi = 6.54$ THz is the transverse optical phonon frequency, and the plasma frequency is $\omega_p^2 = 4\pi Ne^2/m^* \epsilon_{\infty}$. The optical effective mass (m^*) accounts for the nonparabolic conduction band of InAs, which becomes more important as the doping density (N) increases.¹⁶ The mass of the donor ions is taken to be infinite. Results of this calculation are shown in Fig. 2 with solid lines. The filled circles are from the THz spectra of six different n -doped samples.

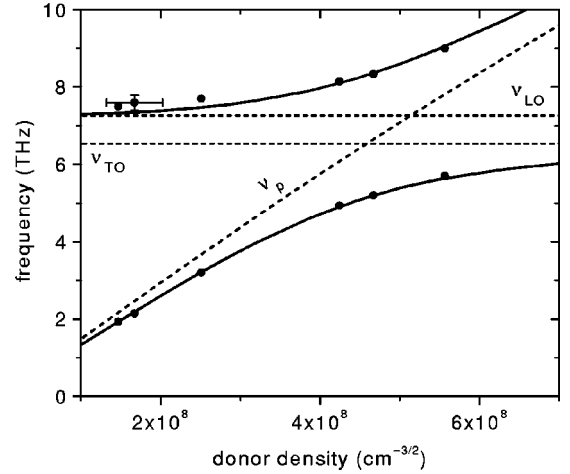


FIG. 2. Dispersion of the plasmon-phonon modes of InAs as a function of donor doping. Filled circles are from experiment; solid curves are derived from Eq. (1).

The center frequencies of the spectral peaks do not change as the optical excitation power is varied by a factor of 3, showing the coherent oscillations are independent of the level of photocarrier injection. This is in agreement with previously reported results on THz emission by cold plasmons in GaAs (Ref. 6) and InSb.⁷ The excitation pulses are p polarized and the detected signals exhibit no dependence on azimuthal rotation for either (100) or (111) InAs samples. This indicates the oscillations are initiated by ultrafast screening of the surface field by optically injected carriers, a mechanism that is well known for GaAs.¹⁰ Recent REOS measurements of coherent phonons in InAs are also consistent with displacive excitation by surface field screening.¹¹

The absorption depth of the pump light is >200 nm, which causes uniform screening of the surface accumulation field (depth ≈ 5 nm, Ref. 17) and also penetrates into the neutral bulk region, i.e., the region where the coherent oscillations originate. We estimate the optically excited carrier density in the pump absorption region to be well in excess of 10^{18} cm^{-3} . This is at least an order of magnitude greater density than the background doping concentration, yet the optically injected electron-hole pairs do not affect the frequency of the cold plasma oscillations in our THz spectra. Absence of a coherent contribution from the photocarriers is due to their inhomogeneous (i.e., quasiexponential) distribution in the bulk region adjacent to the surface.¹⁸

A quantitative understanding of the THz signals is obtained with the time-domain model of Ref. 9, which couples the electronic polarization with the lattice displacement. Fourier analysis gives the power spectrum of the emitted radiation

$$P(\omega) \propto \omega^4 |E(\omega)|^2 \times \left| \frac{\omega_p^2 (\epsilon_{\infty} D_1(\omega) - 4\pi\Omega) + \Omega [D_2(\omega) - \omega_p^2]}{\epsilon_{\infty} D_1(\omega) D_2(\omega) - 4\pi\Omega \omega_p^2} \right|^2, \quad (2)$$

$$D_1(\omega) = -\omega^2 + i\gamma_{ph}\omega + \omega_{\text{LO}}^2,$$

$$D_2(\omega) = -\omega^2 + i\gamma_{el}\omega + \omega_p^2$$

with $\omega_{LO} = 2\pi\nu_{LO}$ and $\Omega = \omega_{TO}^2(\epsilon_o - \epsilon_\infty)/4\pi$. The electric field transient at the edge of the space-charge layer is modeled as $E(t) = E_o[\tanh(t/\tau) + 1]$, where τ accounts for the response time of the surface field screening. This function is an analytic approximation to the calculated surface field dynamics.^{6,14,19} The Fourier transform of $E(t)$ gives the spectrum of the surface transient $|E(\omega)|^2 \propto \text{csch}^2(\pi\omega\tau/2)$, for $\omega > 0$. The width of the accumulation layer scales approximately as $1/\sqrt{N}$ so we expect faster screening as the donor density increases.²⁰ The bare phonon relaxation time is set at $1/\gamma_{ph} = 2$ ps reflecting its anharmonic decay²¹ and best fits to the experimental data are obtained with a density-independent plasmon damping time (i.e., electron momentum relaxation time) of $1/\gamma_{el} = 125$ fs. Results of the model calculations are depicted by dotted curves in Fig. 1(b). The surface field screening response times are found by fitting the amplitude of the upper-hybrid mode peaks, yielding values of $\tau = 76, 68, 58,$ and 52 fs for the increasing sequence of doping densities.

In the strong coupling regime, the phononlike mode takes on the damping rate of the plasmons while the plasmons become more phononlike.²² Most experiments—in particular time-resolved Raman measurements—study the behavior of just one mode and deduce mode hybridization indirectly.²³ Here, we can clearly resolve the spectra of both modes as a function of coupling and directly address this question. It is seen that the contribution of the phononlike mode to the radiated THz signal depends critically on the spectral proximity of the plasma frequency. When the modes are strongly coupled, the lattice dynamics can significantly affect the electric field that is responsible for the emitted radiation. We believe our data represents the first observation of this effect, which was predicted in Ref. 9.

We now discuss the spectral linewidths in Fig. 1(b). The decay of weakly coupled coherent plasmons is associated with the electron momentum relaxation time and therefore the mobility of the semiconductor. As with GaAs, the mobility of room temperature InAs should be dominated by LO phonon scattering.¹⁴ The plasmon damping rate derived from our experiments is, however, about 3 times higher than indicated by Hall mobility measurements. THz interferograms at 80 K (not shown) reveal that this unexpectedly high plasmon damping rate does not change when compared to room temperature spectra. Because LO phonon scattering is strongly temperature dependent, it must therefore play a minor role here. A constant plasmon damping rate is used in the model and fits the spectra well at all doping densities, which shows that ionized impurity scattering is negligible. Nonuniform spatial excitation of the coherent volume due to the transverse laser profile can cause inhomogeneous broadening,^{9,24} but we found the plasmon line shape to be insensitive to spatial filtering of the THz beams. Landau damping can be ruled out because large wave vector modes do not efficiently radiate.¹⁴ If the coherent plasmons are confined in the surface accumulation region ($q \geq 2 \times 10^6 \text{ cm}^{-1}$) as observed in REOS, single particle excitation could take place and the plasmons would be severely broadened by Landau damping accompanied by strong emission at the bare LO phonon frequency.^{16,25} We find no peaks at the LO phonon frequency

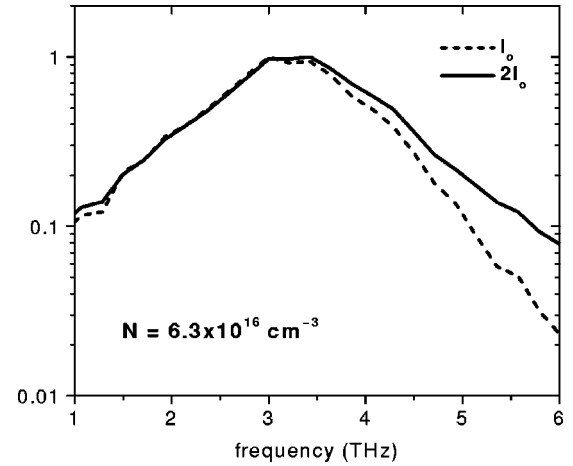


FIG. 3. Line shape of the plasma peak at two different excitation levels. The solid curve is obtained at approximately twice the irradiance of the dashed curve.

in the THz spectra of the samples n -doped at 1.8×10^{17} and $3.1 \times 10^{17} \text{ cm}^{-3}$. It can be concluded that longitudinal modes with wave vector $q \approx 0$ are emitted, with a corresponding plasmon displacement amplitude of at least 50 nm. The long-wavelength nature of the radiating modes means that Landau damping of the coherent plasmons is not relevant.

The high plasmon damping rate is explained by the presence of hot carriers ($h\nu_{laser} - E_g \approx 1.2 \text{ eV}$) injected by the near-infrared pump pulse. Although the inhomogeneous longitudinal distribution of the photocarriers does not contribute to the coherent signals, previous work has revealed that there can be significant damping of coherent plasmons and phonons due to scattering with optically generated electrons and holes.^{18,22–24,26} To confirm the presence of strong scattering by nonequilibrium carriers, the excitation irradiance of the near-infrared pump light is increased by about a factor of 2, leading to a larger photocarrier density in the radiating volume beneath the surface accumulation layer. Changes in the THz spectrum in the vicinity of the coherent plasmon for the sample doped $6.3 \times 10^{16} \text{ cm}^{-3}$ are depicted in Fig. 3. With higher photocarrier density (solid line), we observe inhomogeneous broadening on the high-frequency side of the plasmon peak. Moreover, the model described by Eq. (2) assumes homogeneous broadening and thus the calculated curves consistently underestimate the experimental spectra on the high-frequency wings of the peaks in Fig. 1(b). This strongly indicates inhomogeneous broadening by optically injected electron-hole pairs is an important factor in the interpretation of our data. The extracted plasmon damping time of $1/\gamma_{el} \sim 125$ fs is also consistent with cold electrons scattering with holes of a much higher density.²⁷ Note that the hot electron-hole distribution induced by above-bandgap laser pulses persists for 3–4 ps in InAs, i.e., longer than the time scale of our measurements.²⁸

In summary, we have studied the emission of far-infrared electromagnetic transients from bulk InAs with a high frequency, uniform bandwidth detection scheme. Distinguish-

able contributions from both coherent plasmons and phonons are observed in the radiated signals. By varying the donor doping and hence the plasma frequency, the long range Coulomb coupling of the electronic polarization with the polar lattice changes, resulting in striking variation of the emission spectra. A nonequilibrium electron-hole plasma injected by

the excitation laser pulse is primarily responsible for damping the coherent oscillations.

Funding provided by the Air Force Office of Scientific Research. M.S.B. gratefully acknowledges the support of NSF through Grant No. ECS-0100636.

-
- ¹A. Mooradian and G.B. Wright, Phys. Rev. Lett. **16**, 999 (1966).
²E. Gornik and R. Kersting, in *Semiconductors and Semimetals*, edited by K. T. Tsen (Academic, San Diego, 2001), Vol. 67.
³T. Dekorsy *et al.*, Phys. Rev. Lett. **74**, 738 (1995).
⁴A. Leitenstorfer, S. Hunsche, J. Shah, M.C. Nuss, and W.H. Knox, Phys. Rev. Lett. **82**, 5140 (1999).
⁵M. Tani *et al.*, J. Appl. Phys. **83**, 2473 (1998).
⁶R. Kersting, K. Unterrainer, G. Strasser, H. Kauffmann, and E. Gornik, Phys. Rev. Lett. **79**, 3038 (1997).
⁷P. Gu, M. Tani, K. Sakai, and T.R. Yang, Appl. Phys. Lett. **77**, 1798 (2000).
⁸J.N. Heyman *et al.*, Phys. Rev. B **64**, 085202 (2001).
⁹A.V. Kuznetsov and C.J. Stanton, Phys. Rev. B **51**, 7555 (1995).
¹⁰T. Dekorsy, G. C. Cho, and H. Kurz, in *Light Scattering in Solids VIII*, edited by M. Cardona and G. Güntherodt (Springer-Verlag, Berlin, 2000).
¹¹H. Kamioka, S. Saito, and T. Suemoto, J. Lumin. **87-89**, 923 (2000).
¹²S. Kono, M. Tani, P. Gu, and K. Sakai, Appl. Phys. Lett. **77**, 4104 (2000).
¹³A. Leitenstorfer, S. Hunsche, J. Shah, M.C. Nuss, and W.H. Knox, Appl. Phys. Lett. **74**, 1516 (1999).
¹⁴R. Kersting, J.N. Heyman, G. Strasser, and K. Unterrainer, Phys. Rev. B **58**, 4553 (1998).
¹⁵S.L. Chuang, S. Schmitt-Rink, B.I. Greene, P.N. Saeta, and A.F.J. Levi, Phys. Rev. Lett. **68**, 102 (1992).
¹⁶M.P. Hasselbeck and P.M. Enders, Phys. Rev. B **57**, 9674 (1998).
¹⁷T.D. Veal and C.F. McConville, Phys. Rev. B **64**, 085311 (2001).
¹⁸T. Dekorsy, H. Auer, H.J. Bakker, H.G. Roskos, and H. Kurz, Phys. Rev. B **53**, 4005 (1996).
¹⁹The surface field transient $E(t)$ can be modeled by other functions, e. g., $\text{erfc}(t/\tau)$, which give similar results.
²⁰T. Dekorsy, T. Pfeifer, W. Kütt, and H. Kurz, Phys. Rev. B **47**, 3842 (1993).
²¹E.D. Grann, K.T. Tsen, and D.K. Ferry, Phys. Rev. B **53**, 9847 (1996).
²²G.C. Cho, T. Dekorsy, H.J. Bakker, R. Hövel, and H. Kurz, Phys. Rev. Lett. **77**, 4062 (1996).
²³F. Vallée, F. Ganikhanov, and F. Bogani, Phys. Rev. B **56**, 13 141 (1997).
²⁴M. Hase *et al.*, Phys. Rev. B **60**, 16 526 (1999).
²⁵Y.B. Li, I.T. Ferguson, R.A. Stradling, and R. Zallen, Semicond. Sci. Technol. **7**, 1149 (1992).
²⁶G.O. Smith, T. Juhasz, W.E. Bron, and Y.B. Levinson, Phys. Rev. Lett. **68**, 2366 (1992).
²⁷R. Hopfel, J. Shah, and S. Juen, in *Hot Carriers in Semiconductor Nanostructures*, edited by J. Shah (Academic, San Diego, 1992).
²⁸H. Nansei, S. Tomimoto, S. Saito, and T. Suemoto, Phys. Rev. B **59**, 8015 (1999).